Accepted Manuscript

Comparison of performance, microorganism populations, and bio-physiochemical properties of granular and flocculent sludge from denitrifying phosphorus removal reactors

Yayi Wang, Xuxin Jiang, Hong Wang, Gang Guo, Jianhua Guo, Jian Qin, Shuai Zhou

PII: S1385-8947(14)01261-3
DOI: http://dx.doi.org/10.1016/j.cej.2014.09.065
Reference: CEJ 12683

To appear in: *Chemical Engineering Journal*

Received Date: 2 February 2014
Revised Date: 18 September 2014
Accepted Date: 20 September 2014

Please cite this article as: Y. Wang, X. Jiang, H. Wang, G. Guo, J. Guo, J. Qin, S. Zhou, Comparison of performance, microorganism populations, and bio-physiochemical properties of granular and flocculent sludge from denitrifying phosphorus removal reactors, *Chemical Engineering Journal* (2014), doi: http://dx.doi.org/10.1016/j.cej.2014.09.065

Comparison of performance, microorganism populations, and bio-physiochemical properties of granular and flocculent sludge from denitrifying phosphorus removal reactors

Yayi Wang[a]*, Xuxin Jiang [a], Hong Wang[a], Gang Guo[a], Jianhua Guo[b], Jian Qin[a], Shuai Zhou[a]

*Corresponding author. Tel: +21 65984275; Fax: +21 65984275; E-mail: yayi.wang@tongji.edu.cn

[a]State Key Laboratory of Pollution Control and Resources Reuse, College of Environmental Science and Engineering, Tongji University, Siping Road, Shanghai 200092, P. R. China

[b]Advanced Water Management Centre *(AMWC)*, The University of Queensland, Brisbane, Queensland 4072, Australia

ABSTRACT:

Granule formation frequently occurs in denitrifying phosphorus (P) removal systems. The differences between granules and flocculants, including P removal capacities, bio-physiochemical properties, and microorganism distribution and diversity, are however still poorly understood. Physical and biochemical characteristics of granules and sludge flocs were investigated through two laboratory-scale sequencing batch reactors (SBRs). One reactor was operated as a flocculent SBR and the other

was operated as a granular SBR, using a granule diameter of 1.92 ± 0.78 mm. Granular sludge had a higher tolerance to inhibitors (nitrite/free nitrite acids (FNAs)), and a higher percentage of P accumulating organisms (PAOs) (72 % vs. 64 % in flocs) than flocculent sludge. The granule crush tests and higher PAOII (unable to use nitrate as an electron acceptor) to PAOs ratios (over 72 %) by fluorescent *in situ* hybridization showed that in both reactors, glycogen accumulating organisms (GAOs) were mainly responsible for nitrate to nitrite reduction, and PAOII further reduced nitrite to nitrogen gas in association with anoxic P uptake; GAOs wash-out weakened the mutual relationship between GAOs and PAOII to some extent, which made denitrification of nitrate to nitrite inefficient and weakened subsequent anoxic P removal. GAOs existed mainly on the surface of the granules, whereas PAOs (PAOI+PAOII) were distributed both on the surface and in the interior of the granules. Thus, GAOs had easier access to carbon sources but were at risk of suffering from exposure to FNA.

Keywords: Denitrifying phosphorus removal; Granule; Extracellular polymeric substances; Diffusion resistance; Microbial community structure; Nitrite

1. Introduction

Denitrifying phosphorus (P) accumulating organisms (DPAOs) have received much attention because of their many advantages, including effective use of organic carbon substrates and low sludge production [1,2]. DPAOs are enriched under

alternating anaerobic and anoxic conditions and are capable of using nitrate (NO_3^--N) or nitrite (NO_2^--N) as electron acceptors instead of oxygen to achieve satisfactory phosphate uptake and nitrogen (N) removal at the same time [2]. This, however, frequently leads to the accumulation of nitrite/free nitrous acids (FNAs) in DPAOs systems when the denitrification process is interrupted [3]. Nitrite and FNAs are toxic to a wide range of microorganisms, and PAOs are sensitive to FNAs at concentrations as low as 0.0017 mg NO_2^--N/L [3,4]. The fact that P accumulating organism (PAO) activities tend to be inhibited by nitrite or FNAs makes the DPAOs process less stable than that of conventional biological P removal (BPR) systems [3], and is a challenge for the practical application of denitrifying P removal technology.

Granular sludge has been proposed as a promising technology for biological wastewater treatment. It has been successfully formed in sequencing batch reactors (SBRs) designed for denitrifying P removal [1,5]. There are many advantages associated with the use of biogranulation technologies in wastewater treatment, including high biomass retention, strong microbial structures, the ability to withstand high-strength wastewater, shock loadings, and also a high tolerance to toxicity [6,7]. If DPAOs are enriched in granular sludge, it is thought that the constraints of the accumulated nitrite or FNA might be eliminated, primarily owing to (i) the dense distribution of biomass at the outer layer of the granular sludge, and (ii) the thicker, extracellular polymeric substance (EPS) matrix that is built up by biofilm cells, which means that granules are more resistant to hazardous materials (e.g., nitrite /FNA) [6]. These unique structural and bio-chemical properties of granular sludge

protect the functional organisms from the harsh external environment, and hence help maintain efficient nutrient removal and the stability of the processes. Further, if DPAOs granules build up a good resistance to nitrite/FNA, it may be possible to use nitrite as an acceptor instead of nitrate. Thus, the denitrifying P removal can be coupled with short-cut nitrification, which will result in more cost-effective and sustainable nutrient removal systems.

Glycogen-accumulating organisms (GAOs) are recognized as the main competitors to PAOs in BPR systems. They take up carbon sources under anaerobic conditions but do not contribute to P removal. If GAO numbers increase, they can cause BPR failure [2]. A new method for separating PAOs from GAOs has been proposed from tests of granular sludge technology in lab-scale SBRs [8]. As PAOs accumulate high amounts of poly-P after aerobic/anoxic P uptake reactions, the settling velocity for PAO-dominated granules is higher than that of GAO-dominated granules. This means that biomass can be segregated by selectively removing sludge at different heights in a granular sludge bed. Using this method, competition between PAOs and GAOs can be controlled, and so it is a good method for manipulating P removal-related microbial populations.

Our current understanding of denitrifying P accumulating microbial granules has been gathered from studies of P removal in aerobic granules [1,5]. To date, there is limited information available about the micro-scale characteristics of denitrifying P accumulating granules in an anaerobic/anoxic/aerobic SBR. Similarly, the differences in (1) denitrifying P removal efficiency, (2) resistance to nitrite/FNA, and

(3) the spatial distribution of organisms between flocs and granules are still unclear. Having this information would help us to better understand the advantages of granules for denitrifying P removal.

This study was therefore conducted to assess how sludge morphology (granules or flocs) affected the performance and microbial community structures of denitrifying P removal systems. We compared the resistance capacity of flocculants and granules with nitrite/FNA through dosing with various concentrations of nitrite. We analyzed the spatial distribution of PAOs and GAOs in granules by fluorescent *in situ* hybridization (FISH). We also examined the properties and PAO-GAO abundances in granules that were crushed through starvation tests to give an improved understanding of the mechanism for anoxic P removal in granules.

2. Materials and methods

2. 1. *The formation of flocs and granular sludge in flocculent SBR (F-SBR) and granular SBR (G-SBR)*

DPAOs biomass was placed in two identical SBRs with a working volume of 7.5 L (an internal diameter of 16 cm and a height of 50 cm) [9] for acclimatization. Both SBRs were fed with synthetic wastewater (composition below) and were operated under alternating anaerobic-anoxic-aerobic conditions. They were operated at room temperature (20 ± 1 °C) with a cycle time of 8 h, which was split into a 15-min filling period, a 120-min anaerobic period, a 210-min anoxic period, a 30-min aerobic period, a 20-min sludge settling period, a 15-min effluent decanting period,

and a 70-min idle phase. During the first 15-min feeding period, 5.5 L of synthetic wastewater was pumped into the reactors, and KNO_3 solution was pulse added into the reactor at the end of the anaerobic period, giving an initial NO_3^--N concentration of 30 ± 6 mg/L.

The rotation (mechanical mixers) speed was controlled at 150 ± 10 rpm during the reaction phases, and the airflow rate was controlled at 40 L/h via a gas-flow controller to keep the dissolved oxygen concentration at about 2–4 mg/L in the post-aerobic phases. Effluent was drawn from the port at 30 cm above the bottom, leaving 2.0 L of mixed liquor in the reactor. The solid retention time (SRT) of the two reactors was approximately 20 days. One hundred and twenty five microliters of mixed liquor was removed at the end of each aerobic period, and mixed liquid suspended solids (MLSS) were maintained at 4000 ± 200 mg/L. Liquid samples were collected at the end of the different phases of each cycle every 3 days.

The two SBRs achieved stable removals of phosphate and nitrate after 90 days operation (called Period I). In the subsequent period (called Period II), the rotation speed and aerobic airflow rate in one of the reactors (G-SBR) were increased to 300 rpm and 100 L/h, respectively, to facilitate the formation of granular sludge, while the other one (F-SBR) remained unchanged. After 240 days of operation (called Period IIb), the average diameter of the granules had reached equilibrium at 1.92± 0.78mm, and stable and efficient denitrifying P removal was achieved in the two SBRs. To distinguish with Period IIb, the SBRs operation during days 90–240 was defined as Period IIa.

Cycle tests were conducted weekly by measuring the NH_4^+-N, PO_4^{3-}-P, NO_3^--N, NO_2^--N, volatile fatty acids (VFAs), dissolved N_2O and internal polymers (poly-β-hydroxybutyrate (PHB), poly-β-hydroxyvalerate (PHV), poly-3-hydroxy-2-methylvalerate (PH2MV), and glycogen concentrations every 30 min through the 8-h cycle. At the start of the cycle tests, the sludge in the two SBRs was washed three times with synthetic wastewater without propionate. Nitrogen gas was introduced into the headspace to ensure anaerobic conditions being maintained for P release. pH was continuously monitored online using a pH probe (pH 3310, WTW Inc., Munich, Germany) and was automatically controlled at 7.5 ± 0.1 by manual addition of 0.3 M HCl or 0.3 M NaOH. The MLSS and mixed liquor volatile suspended solids (MLVSS) concentrations were measured at the end of the aerobic phase every week (see section 2. 5).

2. 2. Batch experiments

2. 2. 1. Experiment 1: phosphate, nitrite, and internal polymer transformations and N_2O production with nitrite as an electron acceptor in floc and granular sludges

After mature P-removal granules were formed, we examined the response of the two different sludges (from F-SBR and G-SBR) to nitrite by measuring PO_4^{3-}-P, NO_2^--N, dissolved/gaseous N_2O, poly-β-hydroxyalkanoates (PHA), and glycogen on day 304. Batch experiments were conducted in four identical sealed reactors. These reactors had a working volume of 3.8 L and an overhead space of 0.2 L. At the start of each test, the reactor was first filled with fresh mixed liquor withdrawn from F-SBR and

G-SBR at the end of the post-aeration phase. 2.8 L synthetic water was added to these reactors after the seeded sludge was settled for 30 min (with the volume of approximately 1 L). Nitrogen gas was then introduced for 5 min to ensure anaerobic conditions for P release were maintained. Nitrite was pulse added into the reactors every 30 and 60 min, so that the nitrite concentrations were 5 and 10 mg/L, respectively, after each addition. The four group tests were called F-R_5, F-R_{10}, G-R_5, and G-R_{10}, depending on the sludge sources and the nitrite addition methods. All tests were carried out at 20 ± 1 °C with a cycle of anaerobic (2 h) and anoxic (5 h) reactions. The pH was manually controlled at 7.5 ± 0.1 by adding 0.3 M HCl or 0.3 M NaOH. The MLVSS concentration was measured in triplicate at the end of each test.

2. 2. 2. Experiment 2: phosphate, nitrite, and internal polymer transformations and N_2O production in different layers of the short-term crushed sludge from G-SBR

Granules were crushed to show the spatial distribution of PAOs and GAOs using a 3-day starvation process (at 28 ± 1°C). The starvation process was initiated at the end of the first cycle on day 332, and the rotation speed was increased to 300 rpm. Air was bubbled through the granular sludge for 30 min every 8 h so that microbial activity would continue.

The granular sludge was crushed after the 3-day starvation, which resulted in flocs and granules coexisting in G-SBR. The rotation speed of the mixer was decreased to 80 rpm so that the mixed solid could be segregated, after which 2, 2.5, and 3.0 L of the mixed sludge were sequentially withdrawn from the bottom of the

G-SBR. After settling for 30 min, the settled sludges were transferred to three identical sealed reactors, each with a working volume of 2.5 L and an overhead space of 0.1 L. These three reactors were defined as G-$R_{bot.}$ (the bottom part), G-$R_{mid.}$ (the middle part), and G-$R_{upp.}$ (the upper part). The measured MLSS concentrations were approximately 3.9g/L in G-$R_{upp.}$, G-$R_{mid.}$ and G-$R_{bot.}$ Cycle tests were then conducted to investigate the denitrifying P removal dynamics in the different sludge layers, using the procedure outlined in section 2.1.

2. 3. Synthetic wastewater

The synthetic wastewater used in this study contained (per liter): 257.1 mg CH_3CH_2COONa (300 mg chemical oxygen demand (COD)), 32.9 mg of KH_2PO_4 (7.5 mg of P), 55.3 mg of $K_2HPO_4 \cdot 3H_2O$ (7.5 mg of P), 38.2 mg NH_4Cl; 85.0 mg $MgSO_4 \cdot 7H_2O$, and 10.0 mg $CaCl_2$. Therefore, the ratio of VFAs to influent phosphorus was 10.8 mg C/mg P. Allylthiourea was added to the three batch reactors to inhibit nitrification [10]. The pH of the synthetic wastewater was maintained at 7.5 ± 0.2 by adding $NaHCO_3$.

2. 4. Microbial community analysis by FISH

2.4.1 Microbial community analysis of the floc and granular sludges

FISH was used, as described by Wang et al. [3], to study the population dynamics of PAOs and GAOs in the reactors. In addition, Cy5-labeled Acc-I-444 was used to target PAOI, and FAM-labeled Acc-II-444 was used to target PAOIIA, IIC, and IID

Accumulibacter, respectively [11]. The standard error of the mean value (SE_{mean}) was calculated as the standard deviation divided by the square root of the number of images.

2.4.2 Spatial distribution in granules by FISH

FISH was performed on granular slices. Granule samples were immediately fixed in freshly prepared paraformaldehyde solution (4 % paraformaldehyde in phosphate-buffered saline (PBS), pH 7.2) at 4 °C for 18 h and subsequently washed in PBS for the microbial distribution analysis in granules. A 20-mm-thick granule section was prepared from a frozen granule sample embedded in an OCT compound (Miles; Elkhart, IN, USA) using a cryostat (CM 3050; Leica, Germany) at –20 °C. Each slice was placed in hybridization wells on a gelatin-coated microscopic slide and immobilized by air drying and dehydrating in a graded series of ethanol (50 %, 80 %, and 98 %). Samples were then hybridized with the probes as mentioned above.

2. 5. Sampling and analytical methods

Mixed liquor samples were taken using a syringe and were immediately filtered through Millipore filter units (0.45 µm pore size) for NH_4^+-N, NO_3^--N, NO_2^--N, PO_4^{3-}-P, COD, and total phosphorus analysis [12]. Analysis methods for glycogen, PHA, and VFAs have been described in Wang et al. [9]. PHA in the samples were calculated as the sum of the measured PHB, PHV, and PH2MV. MLSS and MLVSS were measured using standard methods [12]. The free nitrous acid (FNA)

concentration was calculated using the formula $S_{N-NO_2^-}/K_a \times 10^{pH}$, with Ka determined using the formula $e^{-2,300/(273+T)}$ for a given temperature T (°C) [13]. The N_2O concentrations in the gas and liquid phases were measured using the method described in Wang et al. [9]. The detection limitation of N_2O measurement is 0.01 ppm. EPS were extracted by formaldehyde-NaOH using the method described by Liu et al. [14]. The total EPS content was defined as the sum of carbohydrates, proteins, and humic substances. The protein and humic substances in EPS were measured using the modified Lowry method [14]. Image analysis, granule size, and specific gravity of granular sludge were determined using the method described by Su et al. [15].

3. Results and Discussion

3. 1. Performance and sludge morphology of F-SBR and G-SBR

3.1.1 Physical properties and EPS composition of the flocculent and granular sludges from F-SBR and G-SBR

During days 90–240 (Period IIa) (Fig. S1), granular sludge gradually formed in G-SBR (Fig. S2a), the reactor that had the higher mixer rotation speed (i.e., 300 rpm) (Fig. S2), while in F-SBR the mean diameter was 0.2 mm (Table 1). This indicates that the increase in the shear force rate caused larger granules to form in G-SBR [6,7].

The granular sludge in G-SBR had better settling properties (higher settling

velocity and lower SVI_{30}) than the floccular sludge in F-SBR (Table 1). Su et al. [15] reported that the settling velocity and specific gravity were 37 m/h and 1.017, respectively, for an aerobic granular sludge. For this study, the settling velocity and specific gravity were 241 ± 29 m/h and 1.171, respectively, in G-SBR. PAOs, capable of storing poly-P, thrived in G-SBR, leading to an increase in the specific gravity and settling velocity.

The EPS content per VSS in G-SBR was approximately 92.5 % higher than that in F-SBR (Table 1). Previous studies have shown that operational conditions such as high aeration intensities, short settling times, high volume exchange ratios, and toxic substances are favorable for EPS production and granule formation [6]. In the present study, the high EPS production in G-SBR may be due to the stressful culture conditions, including the high shear forces (in Period II) and FNA accumulation (mainly in adaptation Period I) (Fig. S1a and b).

3. 1. 2 Cycle tests under normal reactor operating conditions for the two SBRs

Figure 1 shows typical steady state cycles (on day 272, Period IIb) in F-SBR and G-SBR. The maximum rates of P release and uptake were 76.3 and 10.5 mg P/g VSS·h, respectively, in F-SBR, and 51.5 and 9.6 mg P/gVSS·h, respectively, in G-SBR (Fig. 1e and f). Maximum denitrifying rates were 9.5 and 12.5 mg NO_3^--N /g VSS·h in G-SBR and F-SBR, respectively (Fig. 1a and B). The low denitrification rate observed in G-SBR can be attributed to the limitations on nitrate transfer to the biomass within the granules. The different maximum denitrifying rates also contributed to the different maximum NO_2^--N accumulations in the two SBRs, i.e.,

0.11 mg/L in F-SBR and 0.56 mg/L in G-SBR. It seems that the granular sludge did not have a higher denitrifying rate (i.e., microbial activity).

During anaerobic phases, the trend in VFA uptake was similar for the two cycles, in that VFAs were completely depleted within 15 min in F-SBR and 30 min in G-SBR (Fig. 1e and f). The amount of PHA synthesis per VFA uptake (PHA/VFA) was almost equal in F-SBR and G-SBR (Table 2). During the sequential anoxic phases, the maximum rates of PHA degradation in F-SBR (8.8 mmol C/L·h) were higher than in G-SBR (5.4 mmol C/L·h). Moreover, the amount of NO_3^--N reduction in F-SBR (31.4 mg/L) was greater than in G-SBR (26.8 mg/L) (Fig. 1a and b). This suggests that there may have been greater constraints on nitrate diffusion to biomass within the granules than flocs, resulting in lower PHA degradation dynamics in G-SBR than in F-SBR. The lower PHA degradation further resulted in lower denitrification and P removal efficiencies in G-SBR than in F-SBR (Fig. 1a, b, e and f), although the amount of anaerobically synthesized PHA in the two SBRs was similar (Table 2).

The amount of glycogen that was anaerobically consumed in G-SBR (glycogen consumption per VFA uptake (Gly/VFA) of 0.41 mmol C/mmol C) was higher than that in F-SBR (Gly/VFA of 0.24 mmol C/mmol C). Because glycogen is the sole energy source for VFA uptake by GAOs, GAOs tend to consume more glycogen for uptake per unit VFAs compared with PAOs [2]. Thus, a high GAOs activity for the G-SBR biomass may have been the result of a higher level of anaerobic glycogen use in G-SBR. However, this finding is contrary to the FISH results, for which a higher

PAOs contents was obtained in G-SBR rather than in F-SBR (see section 3.2.1).

3. 2 FISH in the two SBRs and microorganism distribution in the granules

3. 2. 1. FISH in the two SBRs

FISH analysis shows that *Accumulibacter*, bounded with PAOMIX probe, were the dominant organisms and represented 64 % (SE_{mean}=1.5 %) of all the biomass in F-SBR and 72 % (SE_{mean}=1.1 %) in G-SBR (Table 2). *Competibacter-related* GAOs represented approximately 21 % (SE_{mean}=0.5 %) of biomass in G-SBR and 16 % (SE_{mean}=0.7 %) in F-SBR, while Defluvicoccus-related GAOs represented less than 1 % (SE_{mean}=0.4 %) in both SBRs (Table 2).

PAOI can reduce nitrate and perform anoxic P removal simultaneously; from a substrate diffusion point of view, the nitrite produced by PAOI are favor for being further reduced to N_2 by themselves. PAOII can only use nitrite but not nitrate as electron acceptors [11]. In F-SBR and G-SBR, the ratios of PAOII to PAOs were 72 % (SE_{mean}=1.4 %) and 76 % (SE_{mean}=0.9 %), respectively. This means that the main mechanism of DPAOs denitrification in the present study was via nitrite reduction. The fact that PAOII rather than PAOI was the dominant PAO subgroup in both of the SBRs suggests that other organisms (e.g., DGAOs) might be responsible for reducing nitrate to nitrite, which could then be used by PAOII for anoxic phosphate uptake.

3. 2. 2. Microorganism spatial distribution in the granules

The FISH images of granule slices showed that GAOs were mainly found near the

granule surfaces (at approximately 0–400 μm from the outer layer), whereas PAOs were found near the surface of the granules and also in the inner layer of the granules (Fig. 2a). Similar results were also reported by Naohiro et al. [17] who found that PAOs existed in both the outer and inner (anaerobic/oxic) layers of the granular sludge. GAOs therefore were able to absorb substrates (i.e., VFA) more easily, but also were more susceptible to suffering from higher FNA exposure. These two opposite effects controlled the number of GAOs and enabled GAOs not to become the dominant microorganisms in G-SBR (Table 2). The exact mechanism controlling spatial variation between PAOs and GAOs in granules remains unclear. It may be related to the different metabolisms of GAOs and PAOs, especially in the starvation cases (details see section 3.5).

3. 3. Anoxic metabolism characteristics of floc and granular sludges using nitrite as an electron accepter

As mentioned in sections 3. 1. 2 and 3. 2. 1, in G-SBR and F-SBR, PAOII dominated in PAOs and there was almost no nitrite accumulations in the stable cycles (Fig. 1a and b). This made it possible to achieve high nitrite reduction rates and resulted in more suitable conditions for N removal via the nitrite pathway. When granular sludge has a higher tolerance to nitrite, N removal via the nitrite pathway will be increasingly common in granular sludge, driven by energy and carbon savings [18]. Therefore, the nitrite shock tests designed for F-SBR and G-SBR sludges focused on anoxic metabolisms of DPAOs.

3. 3. 1. Comparison of the denitrifying P removal efficiency

When fed with nitrite as electron acceptors, the denitrifying and P uptake rates in the anoxic batch tests were much lower than those observed in typical cycles (Fig. 4 and 1). This can be due to the inhibitory effect of high nitrite concentrations produced in the anoxic batch experiments (i.e., higher nitrite accumulations did not occur in typical cycles). The maximum FNA concentrations reached 0.4 and 0.8 μg HNO_2-N/L, respectively, in F-R_5/G-R_5 and F-R_{10}/G-R_{10}, with the maximum NO_2^--N concentrations of 5 and 10 mg/L, respectively. These higher FNA concentrations might have inhibited P uptake, as an FNA concentration of 0.7 μg HNO_2-N/L was previously reported to cause a sharp decrease in the P uptake rate [18].

In the 5-h anoxic reaction, the total NO_2^--N reduction in F-R_5 was 50 and 37 mg N/L in G-R_5. The difference in the NO_2^--N reduction rates led to the further different N_2O accumulation rates observed in F-R_5 (26 mg N_2O-N/L) and G-R_5 (7 mg N_2O-N /L) (Fig. 3a and c), which represented 54 % and 19 % of the reduced NO_2^--N, respectively, at the end of the anoxic phases. When compared with F-R_5 and G-R_5, the denitrifying efficiencies in F-R_{10} and G-R_{10}, were 24 % and 16 % lower, respectively. N_2O accumulation reached 58 % and 54 % of the reduced NO_2^--N, owing to the higher inhibition by FNA. Previous studies have also reported that FNA inhibits the activity of nitrous oxide reductase (Nos), which causes the accumulation of N_2O in denitrification processes [19].

The anoxic P uptake was higher in F-R_5 (53 mg PO_4^{3-}-P/L) than in G-R_5 (36 mg PO_4^{3-}-P /L) (Fig. 3e-h). In F-R_{10} and G-R_{10}, P uptake was 20 and 26 mg PO_4^{3-}-P/L,

respectively. Compared with F-R_5 and G-R_5, the P removal efficiencies in F-R_{10} and G-R_{10} were 62 and 28 % lower, respectively. These findings demonstrate that, with the low NO_2^-/FNA (e.g., 5 mg NO_2^--N/L), microbial activities were still higher in the floc sludge than in the granular sludge; however, after the NO_2^-/FNA ratio increased to a certain level (e.g., 10 mg NO_2^--N /L in the present study), the granular sludge system exhibited a stronger tolerance to the inhibitor (i.e., nitrite/FNA). This observation is consistent with former studies, and confirms that biogranulation technologies are able to withstand high-strength wastewater and shock loadings, and are tolerant to toxicity [6,7].

At higher nitrite/FNA ratios (i.e., 10 mg NO_2^--N /L), the ratios of $P_{uptake}/NO_2^-N_{reduction}$ for the flocs and granules decreased from 1.1 to 0.5 mg P/mg N, and from 1.0 to 0.8 mg P/mg N, respectively (Fig. 3). Clearly, a relatively higher $P_{uptake}/NO_2^-N_{reduction}$ ratio was still maintained by G-SBR after being exposed to higher nitrite/FNA. In the granules, the concentration gradient of the nitrite/FNA ratio decreased from peripheral to central granules. Because GAOs were mainly on the surface of the granules (Fig. 2a and b), nitrite/FNA presented a more direct and distinct inhibitory effect on GAOs than on PAOs. Therefore, PAOs activity was sustained at a higher level than that of GAOs, which in turn contributed to the higher $P_{uptake}/NO_2^-N_{reduction}$ [20] in granules even with higher nitrate/FNA exposure. If granules have a dense structure, the obstructive reaction caused by hazardous substances can be avoided, which protects some sensitive microorganisms (e.g., PAOs) from negative impacts and hence improves the operating stability of DPAO

systems.

3. 3. 2. Effect of FNA on PHA consumption and glycogen production during anoxic phases

When fed with nitrite, PHA consumption and glycogen production decreased in all reactors during the anoxic phases. Moreover, nitrite/FNA posed greater constraints on internal polymer transformations in floc sludge than in granular sludge (Fig. 3e–h). The PHA consumption was 48 % and 13 % lower in F-R_{10} and G-R_{10} than in F-R_5 and G-R_5, respectively, and the glycogen production reduced by 100% and 62%, respectively. Interestingly, glycogen consumption even occurred anoxically in F-R_{10}, indicating that glycogen was degraded to supply energy in the case of FNA inhibition (ATP production process was inhibited by FNA).

Above findings showed when nitrite accumulation is low (e.g., under normal SBR operating conditions) or when nitrite additions are low (e.g., adding 5 mg N/L of nitrite), the denitrifying P removal efficiency was higher for flocs than for granules (Fig. 3a, c, e and g). Increasing the nitrite dose to 10 mg N/L, however, resulted in a higher denitrifying P removal efficiency in granules than in flocs, mainly due to the granules being more resistant to nitrite/FNA transfer into the bacterial aggregates (Fig. 3b, d, f and h).

3. 4. Batch experiments for the crushed granular sludge

Batch experiments were conducted on crushed granules, to further confirm the spatial distribution of the functional microorganisms in granules and determine the

roles of GAOs and PAOs (e.g., their cooperative relationship) in the present denitrifying P removal process. Three layers of crushed granules containing floccular and granular sludge were distinguished according to their different settling velocities and densities (Fig. S2c).

3. 4. 1. Changes in EPS contents and settleability of the crushed granules

The granular sludge was crushed after 3 days of famine exposure (Fig. S2c), caused by the degradation of EPS, typically used as a carbon and energy source by bacteria during substrate shortages [6]. The EPS content of granular sludge decreased from 336.1 to 147.6 mg/g VSS, representing a decrease of 56 % (data not shown). More specifically, the carbohydrate, protein and humic substance contents were reduced by 48 %, 31 %, and 72 %, respectively, when compared with their contents prior to famine exposure. EPS are fundamental to the structure of microbial aggregates and the interactions between cells, and thus are expected to control the stability of microbial aggregates [16]. Once EPS are removed from the sludge surface, the outer region of the granular sludge is likely to disperse (Fig. 2c) [16], resulting in fewer attached microbial cells and more free microbial cells [21].

The SVI_3 was 15.1 mL/g in G-$R_{bot.}$, compared with 35.7 mL/g in G-$R_{upp.}$ and 25.5 mL/g in G-$R_{mid.}$ (data not shown). This difference in SVI_3 between the three reactors is due to differences in the density and radius of the granules (Fig. S2c).

3. 4. 2. Comparison of the denitrifying phosphorus removal efficiencies

Even though the mass transfer efficiency rate was lower in G-$R_{bot.}$, a higher $P_{release}/VFA_{uptake}$ ratio of 0.36 mmol P/mmol C was still maintained in this reactor

(Table 2). The $P_{release}/VFA_{uptake}$ ratio was 0.30 mmol P/mmol C in G-$R_{upp.}$ and 0.32 mmol P/mmol C in G-R_{mid} (Table 2). These results suggest that there were more active PAOs in G-$R_{bot.}$ where more granules containing inner part of the seeding granules from G-SBR was remained (Oehmen et al., 2006). Compared with maximum P release and uptake rates of 51.5 and 10.5 mg/g VSS·h in G-SBR, the P release rates in these three crushed sludge reactors were higher (Table 3), mostly due to the substrate and nutrients being less resistant to diffusion after the granules were crushed.

During the anoxic phases, concentrations of NO_3^--N decreased by 22.7, 20.7, and 18.3 mg N/L, respectively, in G-$R_{upp.}$, G-$R_{mid.}$, and G-$R_{bot.}$ (Fig. 4a–c). The maximum NO_2^--N accumulations were lower than 0.1 mg/L in all three batch reactors. The corresponding N removal efficiencies were 66.7 % (G-$R_{upp.}$), 60.9 % (G-$R_{mid.}$), and 53.8 % (G-$R_{bot.}$). As expected, the highest ratio for the maximum anoxic P uptake per NO_3^--N reduction (P_{uptake} /$N_{reduction}$) was observed for G-$R_{bot.}$ (Table 3), which confirms that, from the three reactors, the ratio of DPAOs/DGAOs was highest in G-$R_{bot.}$. This finding is consistent with the highest $P_{release}/VFA_{uptake}$ ratio occurring in G-$R_{bot.}$.

The relatively low N removal efficiencies (53.8 %) observed in G-$R_{bot.}$ may be due to the lower cooperative efficiency between DGAOs and PAOII, i.e., the percentage of DGAOs was lower in G-$R_{bot.,}$ which resulted in less efficient nitrate to nitrite reduction than in G-$R_{upp.}$ and G-$R_{mid.}$. The higher denitrification rates, but low P_{uptake} /$N_{reduction}$, observed for G-$R_{upp.}$, indicate that there were more DGAOs in

G-$R_{upp,}$ and that they occupied a niche more efficiently, because DGAOs were the main organisms responsible for nitrate to nitrite reduction, which could subsequently be used by PAOII for anoxic phosphate uptake (Fig. 2b).

3. 4. 3. Transformations of PHA and glycogen for the different layer sludges

There were distinct biochemical transformations in PHA and glycogen in anaerobic phases, comparing to those in anoxic phases (Fig. 4g). In the anaerobic phase, the PHA/VFA ratios were almost equal in G-$R_{upp.}$, G-$R_{mid.}$ and G-$R_{bot.}$ with values of 1.58, 1.55, and 1.60 mmol C/mmol C, respectively (Fig. 4g). However, more glycogen was consumed in G-$R_{upp.}$ during the anaerobic period. The ratio of glycogen hydrolyses per VFA uptake (PHA/VFA) was 0.44 mmol C/mmol C in G-$R_{upp.}$, and was 0.40 and 0.33 mmol C/mmol C in G-$R_{mid.}$ and G-$R_{bot.}$, respectively (Fig. 4g). The higher level of glycogen use observed in G-$R_{upp.}$ implies that GAOs in this reactor may have been more active.

3. 4. 4. Biomass characterization of the different layer sludges

FISH was performed to determine the populations of GAOs and PAOs in the three sludges. *Accumulibacter*-related PAOs dominated in the three sludges, with 56 % (SE_{mean} = 1.5 %), 68 % (SE_{mean} = 1.7 %), and 78 % (SE_{mean}=1.3 %) of the biomass in G-$R_{upp.}$, G-$R_{mid.}$ and G-$R_{bot.}$, respectively. *Competibacter*-related GAOs made up approximately 28 % (SE_{mean} = 0.5 %), 17 % (SE_{mean} = 0.7 %), and 12 % (SE_{mean} = 0.5 %), in G-$R_{upp.}$, G-$R_{mid.}$ and G-$R_{bot.}$, respectively. *Defluvicoccus*-related GAOs made up less than 2.5 % (SE_{mean} = 0.4 %) of the biomass in all three reactors.

The PAO number quantified by FISH supports the observed chemical

transformations, i.e., the highest ratio of $P_{release}/VFA_{uptake}$ occurred in G-$R_{bot.}$ and was linked to the highest ratio of PAOs/GAOs (Table 3). PAOII were the dominant organisms in the three reactors, representing 67 % (SE_{mean} = 1.2 %) of PAOs in G-$R_{upp.}$, 72 % (SE_{mean} = 1.5 %) in G-R_{mid}, and 73.0 % (SE_{mean} = 0.7 %) in G-$R_{bot.}$ The PAOs/GAOs percentage for the different layers of crushed sludge was in good agreement with the FISH results for the granule slices, i.e., there were more GAOs on the surface of the granules and they tended to be crushed from the granules, while PAOs were found both on the surface and inside the granules.

In a previous study of an aerobic granular sludge system [8], to prioritize PAOs over GAOs, the excess sludge was removed mainly from the GAOs-rich top of the sludge bed for SRT control, while minimal proportions of bottom granules were removed. For granular (denitrifying) P removal systems similar to this study, a novel method for crushing granules was proposed and applied to GAOs wash-out easily by removing the upper layer of the crushed granular sludge. Nevertheless, the wash-out of GAOs may reduce the denitrifying P removal efficiency because GAOs played an important role in nitrate reduction in the present two DPAOs SBRs, despite the fact that GAOs are generally considered to be undesirable organisms in BPR processes.

3. 5. Proposed mechanism of microorganism spatial distribution in denitrifying P removal granules

PAOs/DPAOs can use poly-P and/or glycogen to supply energy, while GAOs/DGAOs have no poly-P pool and so can only use glycogen to supply energy

[22]. EPS are a potential energy supply for organisms in starvation situations [6]. GAOs therefore may have a tendency to use EPS rather than PAOs in a starvation scenario, and tend to crush from granules in situations where EPS are consumed as an energy and carbon source for GAOs aggregation [22].

In G-SBR and F-SBR, famine conditions occurred frequently, e.g., in idle phases (210 min per day), during which EPS were able to be used by PAOs and GAOs to supply endogenous energy. High GAO ratios were maintained in the crushed, dispersed EPS layer as GAOs were found on the outer layer of the granules (Fig. 2a and Table 3), and were easily washed out from the system due to their low settling velocity. The higher GAOs ratio in G-$R_{upp.}$ than that in G-R_{bot} in the test of crushed granular sludge strongly supported this speculation (Table 2). This contributed to the unique spatial distribution of PAOs and GAOs and the relatively high percentage of PAOs and GAOs in the granules (Table 1).

Similar to what was proposed by Sheng et al. [16], we suggest that the granules are comprised of two distinct parts, i.e., a dispersible part and a stabile part (Fig. 2c). The stabile part is found in the inner layer of granules and contains biomass in a stable structure tightly glued by EPS, whereas the dispersible part contains dispersible cells loosely held together with EPS [6] in the outer layer of granules (Fig. 2c). The dispersed EPS layer broke down more easily from the granules and coexisted in the mixed sludge. The stabile part of the granules may be made up of PAOs that have denser EPS. GAOs may have less EPS (EPS tends to be consumed to supply energy) and may be dynamically adsorbed and transmitted, and so are

found in the most dispersible part, i.e., the outer layer of the granules (Fig. 2c).

DPAOs granules with a dense structure and a higher EPS content appeared to be more tolerant to higher nitrite/FNA, which could be due to a higher resistance to the transfer of nitrite/FNA into the bacterial aggregates. This suggests that the DPAO granules may be useful for wastewater treatment applications with higher nitrate or nitrite concentrations.

4. Conclusions

DPAO granules with a dense structure and a higher EPS content appeared to be more tolerant to higher nitrite/FNA, which may be due to a higher resistance to the transfer of nitrite/FNA into the bacterial aggregates. This suggests that the DPAO granules may be useful for wastewater treatment applications with higher nitrate or nitrite concentrations. A higher PAOs content was achieved in the granules. Higher PAOII/PAO ratios were achieved in both flocculated and granulated SBRs, and the main mechanism for anoxic P removal was through reduction of nitrate mainly by DGAOs, while further reduction of nitrite (and P uptake) was mainly by PAOII. In granules, PAOs were found near the granule surface and also in the inner part of the granule, whereas GAOs mostly remained near the granule surface. Thus, GAOs were able to absorb substrates (i.e., VFA) more easily, but also were more susceptible to suffering from higher FNA exposure. A novel method for crushing granules was proposed and applied to help understand the mechanism that determined the spatial distribution of PAO-GAOs and the pathway of anoxic P removal in granules.

Acknowledgments

This research was supported by the National Natural Science Foundation of China (NSFC) (nos. 51078283 and 51178325). The Shanghai Science and Technology Committee Rising-Star Tracking Program (12QH1402400) and the Fundamental Research Funds for the Central University (Tongji University) (0400219238) are also acknowledged.

REFERENCES

[1] Bassin, J. P., Kleerebezem. R., Dezotti, M., van Loosdrecht, M. C. M., 2012. Simultaneous nitrogen and phosphate removal in aerobic granular sludge reactors operated at different temperatures. Water Res. 46, 3805–3816.

[2] Zhou, Y., Limb, M., Harjono, S., Ng, W. J., 2012. Nitrous oxide emission by denitrifying phosphorus removal culture using polyhydroxyalkanoates as carbon source. Journal of Environmental Sciences. 24, 1616–1623.

[3] Wang, Y.Y., Gang, G., Wang H., Stephenson, T., Guo, J. H., Ye, L., 2013. Long-term impact of anaerobic reaction time on the performance and granular characteristics of granular denitrifying biological phosphorus removal systems. Water Res. 47, 5326-5337.

[4] Zhou, Y., Ganda, L., Lim, M., Yuan, Z. G., Kjelleberg S., Ng, W. J., 2010. Free nitrous acid (FNA) inhibition on denitrifying polyphosphate accumulating organisms (DPAOs). Applied Microbiology and Biotechnology. 88, 359–369.

[5] Zhou, Y., Pijuan, M., Yuan, Z. G., 2008. Development of a 2-sludge, 3-stage system for nitrogen and phosphorous removal from nutrient-rich wastewater using granular sludge and biofilms. Water Res. 42, 3207–3217.

[6] Sheng, G. P., Yu, H. Q., Li, X., 2010. Extracellular polymeric substances (EPS) of microbial aggregates in biological wastewater treatment systems: A review. Biotechnol. Advan. 28, 882–894.

[7] Seviour, T., Yuan, Z. G., van Loosdrecht, M. C. M., Lin, Y. M., 2012. Aerobic sludge granulation: A tale of two polysaccharides? Water Res. 46, 4803–4813.

[8] Winkler, M. K. H., Bassin, J. P., Kleerebezem, R., de Bruin, L. M. M., van den Brand, T.P.H., van Loosdrecht, M.C.M., 2011. Selective sludge removal in a segregated aerobic granular biomass system as a strategy to control PAO-GAO competition at high temperatures. Water Res. 45, 3291–3299.

[9] Wang, Y. Y., Geng J. J., Ren, Z. J, He, W. T., Xing, M. Y., Wu, M., Chen, S. W., 2011. Effect of anaerobic reaction time on denitrifying phosphorus removal and N_2O production. Bioresour. Technol. 102, 5674–5684.

[10] Oehmen, A., Saunders, A.M., Vives, M.T., Yuan, Z., Keller, J., 2006. Competition between polyphosphate and glycogen accumulating organisms in enhanced biological phosphorus removal systems with acetate and propionate as carbon sources. J. Biotechnol. 123, 22-32.

[11] Flowers, J. J., He, S. M., Yilmaz, S., Noguera, D. R., McMahon, K. D., 2009. Denitrification capabilities of two biological phosphorus removal sludges dominated by different Candidatus Accumulibactert clades. Environ. Microbiol. 1, 583–588.

[12] APHA., 1998. Standard Methods for the Examination of Water and Wastewater, twentieth ed. American Public Health Association, Washington D.C., USA.

[13] Anthonisen, A. C., Loehr, R.C., Prakasam, T. B. S., Srinath, E.G., 1976. Inhibition of nitrification by ammonia and nitrous acid. Res. J. Water Pollut. C 48, 835–852.

[14] Liu, H., Fang, H., 2002. Extraction of extracellular polymeric substances (EPS) of sludges. J. Biotechnol. 95, 249-256.

[15] Su, K. Z.., Yu, H. Q., 2005. Formation and Characterization of Aerobic Granules in a Sequencing Batch Reactor Treating Soybean-Processing Wastewater. Environ. Sci. Technol. 39, 2818–2827.

[16] Sheng, G. P., Yu, H. Q., 2006. Characterization of extracellular polymeric substances of aerobic and anaerobic sludge using 3-dimensional excitation and emission matrix fluorescence spectroscopy. Water Res. 40, 1233–1239.

[17] Naohiro, K., Juhyun, K., Satoshi, T., Ryuichi, S., 2006. Anaerobic/oxic/anoxic granular sludge process as an effective nutrient removal process utilizing denitrifying polyphosphate-accumulating organisms. Water Res. 40, 2303–2310.

[18] Zhou, Y., Oehmen, A., Lim, M., Vadivelu, V., Ng, W. J., 2011. The role of nitrite and free nitrous acid (FNA) in wastewater treatment plants. Water Res. 45, 4672–4682.

[19] Wang Y, Geng J, Guo G, Wang C, Liu S., 2011. N_2O production in anaerobic/anoxic denitrifying phosphorus removal process: The effects of carbon sources shock. Chemical Engineering Journal. 172, 999-1007.

[20] Kuba, T., Smolders, G. J. F., van Loosdrecht, M. C. M., Heijnen, J. J., 1993. Biological phosphorus removal from wastewater by anaerobic and anoxic sequencing batch reactor. Water Sci. Technol. 27, 241–252.

[21] Sand, W., Gehrke, T., 2006. Extracellular polymeric substances mediate bioleaching/biocorrosion via interfacial process involving iron (III) ions and acidophilic bacterial. Res Microbiol. 157, 49–56.

[22] Acevedo, B., Oehmen, A., Carvalho, G., Seco, A., Borra, L., Barat, R., 2012. Metabolic shift of polyphosphate-accumulating organisms with different levels of polyphosphate storage. Water Res. 46, 1889–1900.

Figure captions

Fig. 1. Typical parameters profiles during one cycle in F-SBR and G-SBR (at day 272, period IIb)

Fig. 2. The FISH images of granule slices (Bar=200 μm) (All bacteria - yellow; PAOs - green; GAOs - red) (a); Schematic representation of the denitrifying P removal route in the granular sludge structure (b); A proposed multi-layer structural model for the granular sludge (modified from Sheng et al., [16]) (c).

Fig. 3. Denitrifying P removal efficiency (a-d) and intracellular compound transformations (e-h) with nitrite as an electron accepter (F-R_5 and F-R_{10} were floc sludge systems with once nitrite addition of 5 and 10 mg N/L, respectively; G-R_5 and G-R_{10} were granular sludge systems with once nitrite addition of 5 and 10 mg N/L, respectively)

Fig. 4. Typical cycle tests with different layers of crushed granular sludge from G-SBR (a and b for G-$R_{upp.}$: the upper layer sludge; c and d for G-$R_{mid.}$: the middle layer sludge; e and f for G-$R_{bot.}$: the bottom layer sludge; g: PHA and glycogen transformations for G-$R_{upp.}$, G-R_{mid} and G-$R_{bot.}$)

Table 1 Physical characteristics of the flocs and granular Sludge (at day 298)

	F-SBR (Floc sludge)	G-SBR (Granular Sludge)
Diameter (mm)	0.10 ± 0.05	1.92 ± 0.78
SVI_{30} (mL/g)	25.5 ± 1.7	13.7 ± 1.2
Settling velocity (m/h)	30 ± 7	241 ± 29
Specific gravity	1.012 ± 0.001	1.171 ± 0.001
Carbohydrate (mg/g VSS)	69.7 ± 0.3	90.2± 0.2
Protein (mg/g VSS)	87.3 ± 0.3	211.4 ± 0.5
Humic substance (mg/g VSS)	17.6 ± 0.2	34.5 ± 0.4
Total EPS (mg/g VSS)	174.6± 0.8	336.1± 1.1

Table 2 Comparison of the anaerobic carbon transformations, P release and biomass compositions with literature studies and metabolic model predictions, with propionate as carbon sources

Study	FISH quantification			P/ VFA[a]	Gly/ VFA[b]	PHA/ VFA[b]	PHB/ VFA[b]	PHV/ VFA[b]	PH2MV/ VFA[b]
	Ac (%)	*Co* (%)	*De* (%)						
Carvalho et al. (2007)	76	-	<1	0.40	0.32	0.97	0	0.40	0.57
PAO metabolic models									
Lu et al. (2006)	-	-	-		0.29	1.22	0	0.56	0.66
Oehmen et al. (2005)	63	<1	<1	0.34	0.04	1.23	0	0.56	0.67
GAO metabolic model									
Oehmen et al. (2005)	<1	<1	>96	0	0.70	1.83	0.13	0.71	0.99
This study									
Flocs (F-SBR)	64[c]	21	<1	0.37	0.24	1.48	0.08	0.68	0.72
Granules (G-SBR)	72[d]	16	<1	0.32	0.41	1.54	0.11	0.63	0.80
Crashed granules from G-SBR									
Upper layer (G-$R_{upp.}$)	56	28	<1	0.30	0.44	1.58	0.10	0.63	0.85
Middle layer (G-$R_{mid.}$)	68	17	<1	0.32	0.40	1.55	0.09	0.62	0.83
Bottom layer (G-$R_{bot.}$)	77	12	<1	0.36	0.33	1.60	0.12	0.61	0.87

[a]Units P mmol/C mmol; [b]Units C mmol/C mmol; - No data

[c]The PAOII ratio maintained at 72% in F-SBR;

[d]The PAOII ratio maintained at 76% in G-SBR.

Table 3 Nitrate and P removal in the typical cycles in F-SBR, G-SBR and batch tests

Sludges		Maximum phosphate release /uptake rate* ($mg \cdot gVSS^{-1}h^{-1}$)	Maximum NO_3^--N reduction* rate ($mg \cdot gVSS^{-1}h^{-1}$)	P/N ratio
Flocs sludge (F-SBR)		76.3/10.5	12.5	0.84
Granular sludge (G-SBR)		51.5/9.6	9.5	1.01
G-SBR	$G\text{-}R_{upp.}$	64.4/5.2	7.0	0.74
	$G\text{-}R_{mid.}$	57.3/5.9	3.6	1.64
	$G\text{-}R_{bot.}$	53.7/8.1	3.4	2.4

* Rates and ratios calculated based on the anoxic reactions of first 15 min

Fig. 1

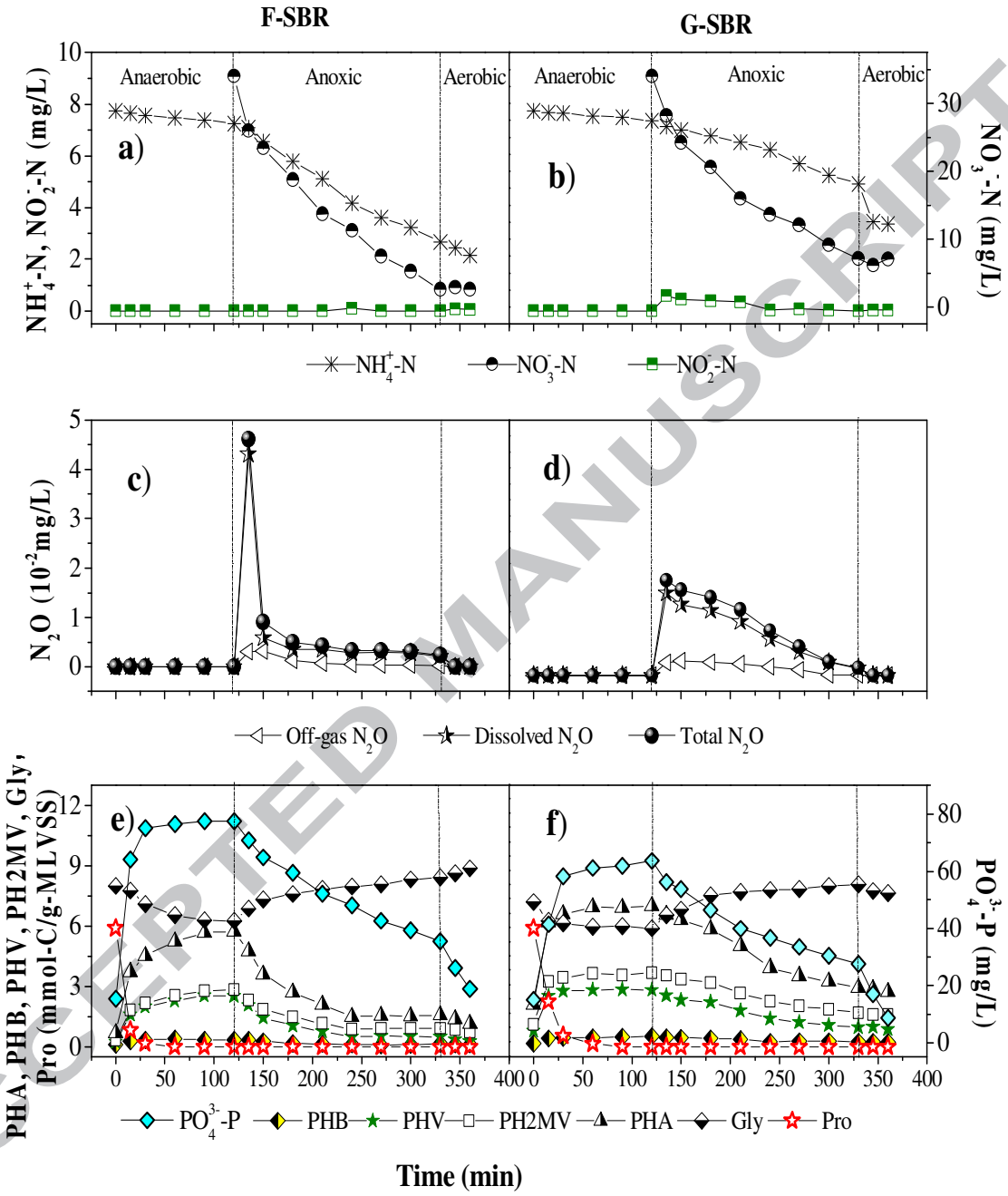

Fig. 2

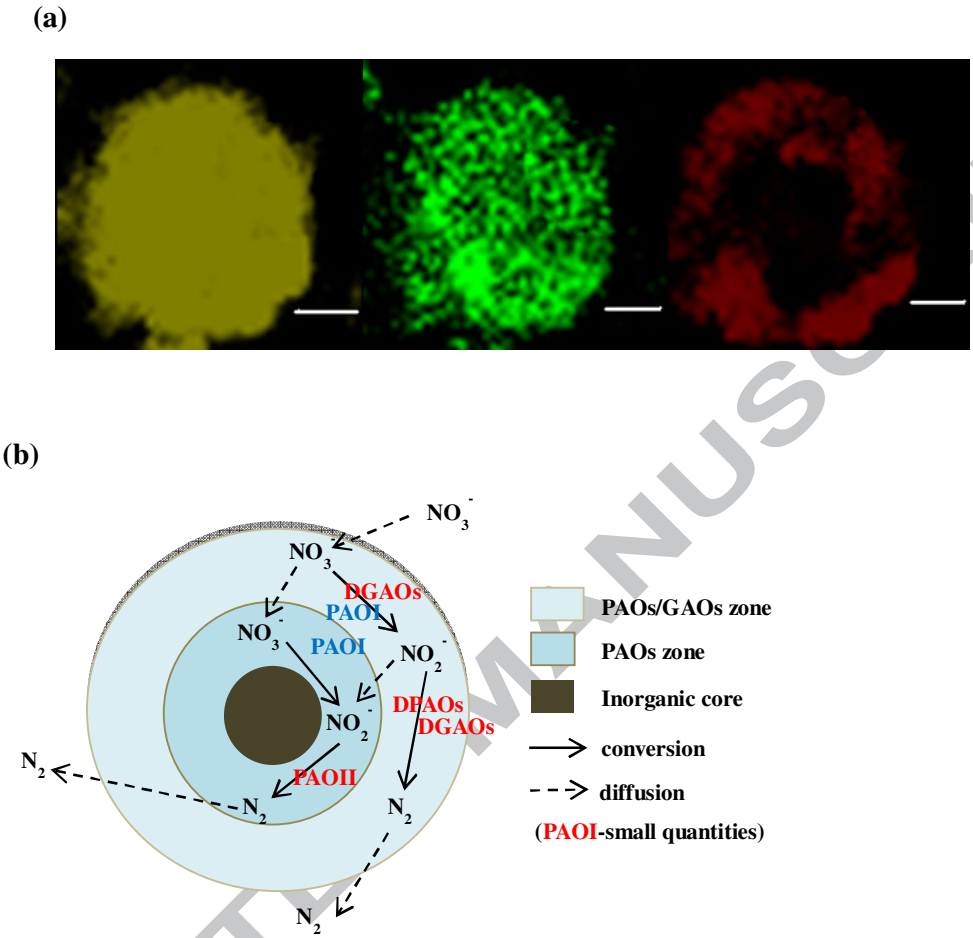

Fig. 3

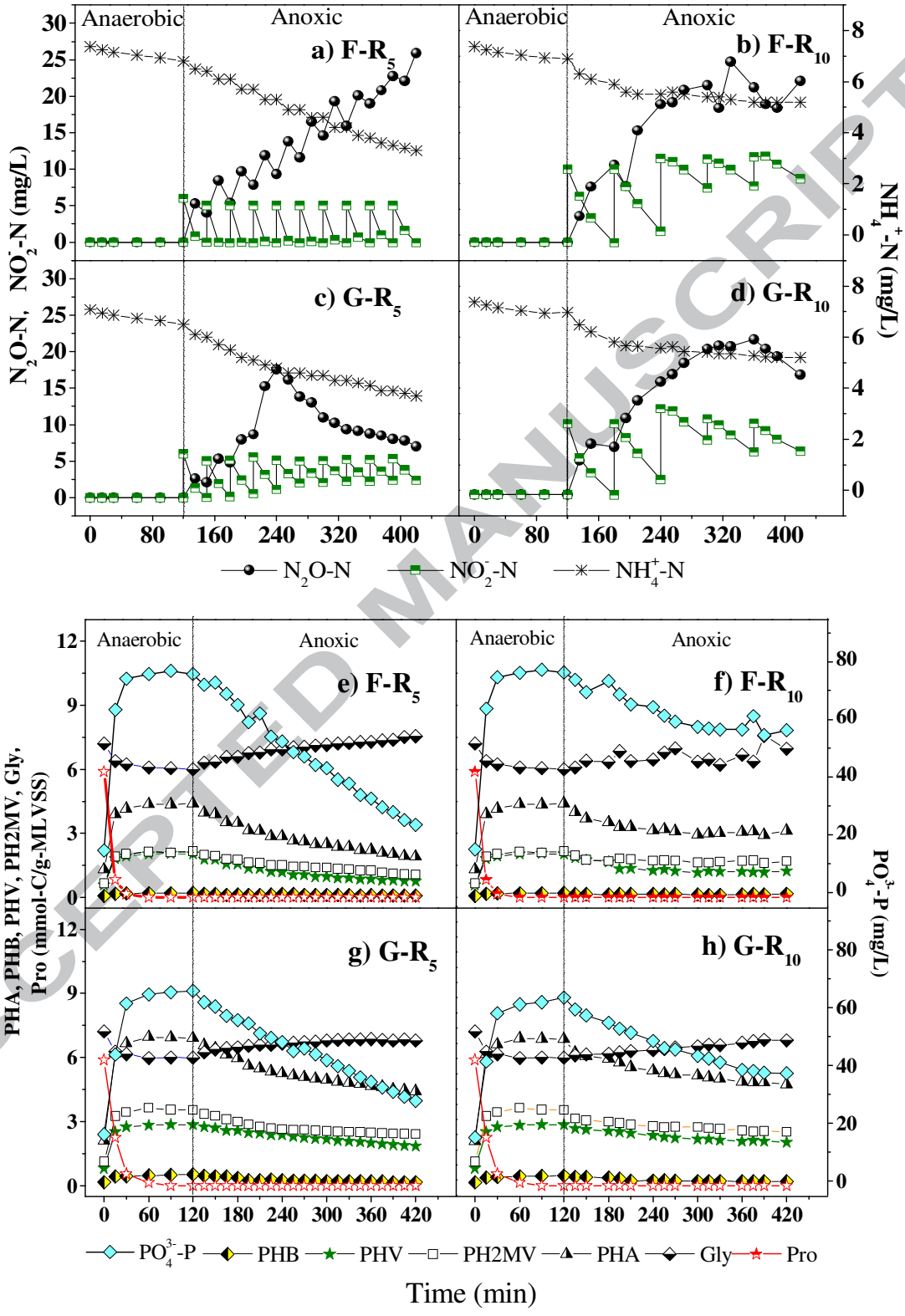

Fig. 4

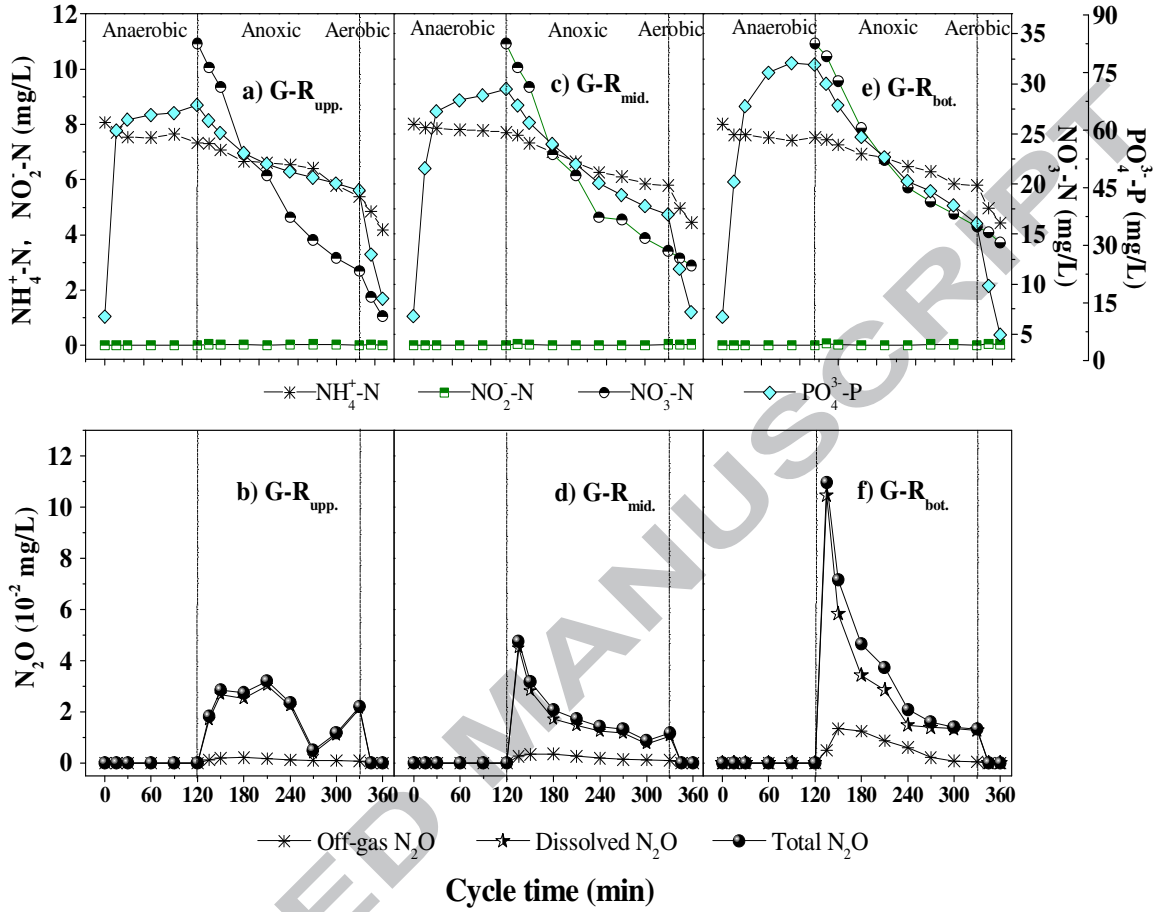

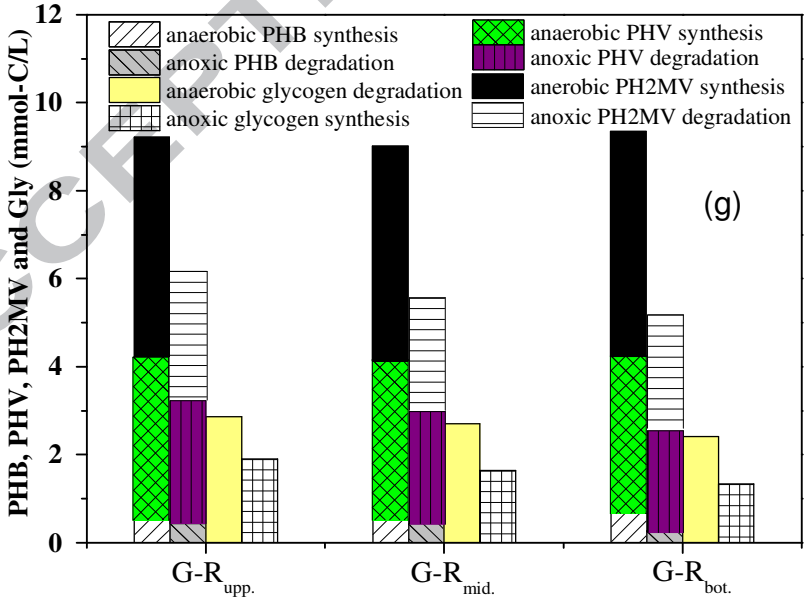

Supporting information

Comparison of performance, microorganism populations, and bio-physiochemical properties of granular and flocculent sludge from denitrifying phosphorus removal reactors

Yayi Wang[a]*, Jiang Xuxin[a], Hong Wang[a], Gang Guo[b], Jianhua Guo[b], Qin Jian[a], Shuai Zhou[a]

*Corresponding author. Tel: +21 65984275; Fax: +21 65984275; E-mail: yayi.wang@tongji.edu.cn

Figure captions

Fig. S1. Long-term variations of nutrient removal efficiency and biomass in F-SBR and G-SBR (a, c, e and g for F-SBR; b, d, f and h for G-SBR).

Fig. S2. Granules and cells on the surface of granules. The images of the mature granular sludge at the end of aerobic phase at day 302 (a); SEM image for the mature granular sludge at day 302 (b); the three parts of crushed sludge from G-SBR (c).

Fig. S3. FISH images (PAOs/GAOs) from the SBRs. Red—*Accumulibacter* (targeted by Cy3-PAOmix probes); Green—*Competibacter* (targeted by Cy5-GAOmix probes). All bacteria are shown in blue—(targeted by FITC-EUBmix probes) (Bar=10 μm).

Fig. S4. FISH images (PAOI/PAOII) from the SBRs. Red—PAOI (targeted by Cy5-Acc-I-444 probes); Green—PAOII (targeted by Cy5-Acc-II-444 probes). All PAOs are shown in blue—(targeted by Cy3-PAOmix probes) (Bar=10 μm).

Fig. S1

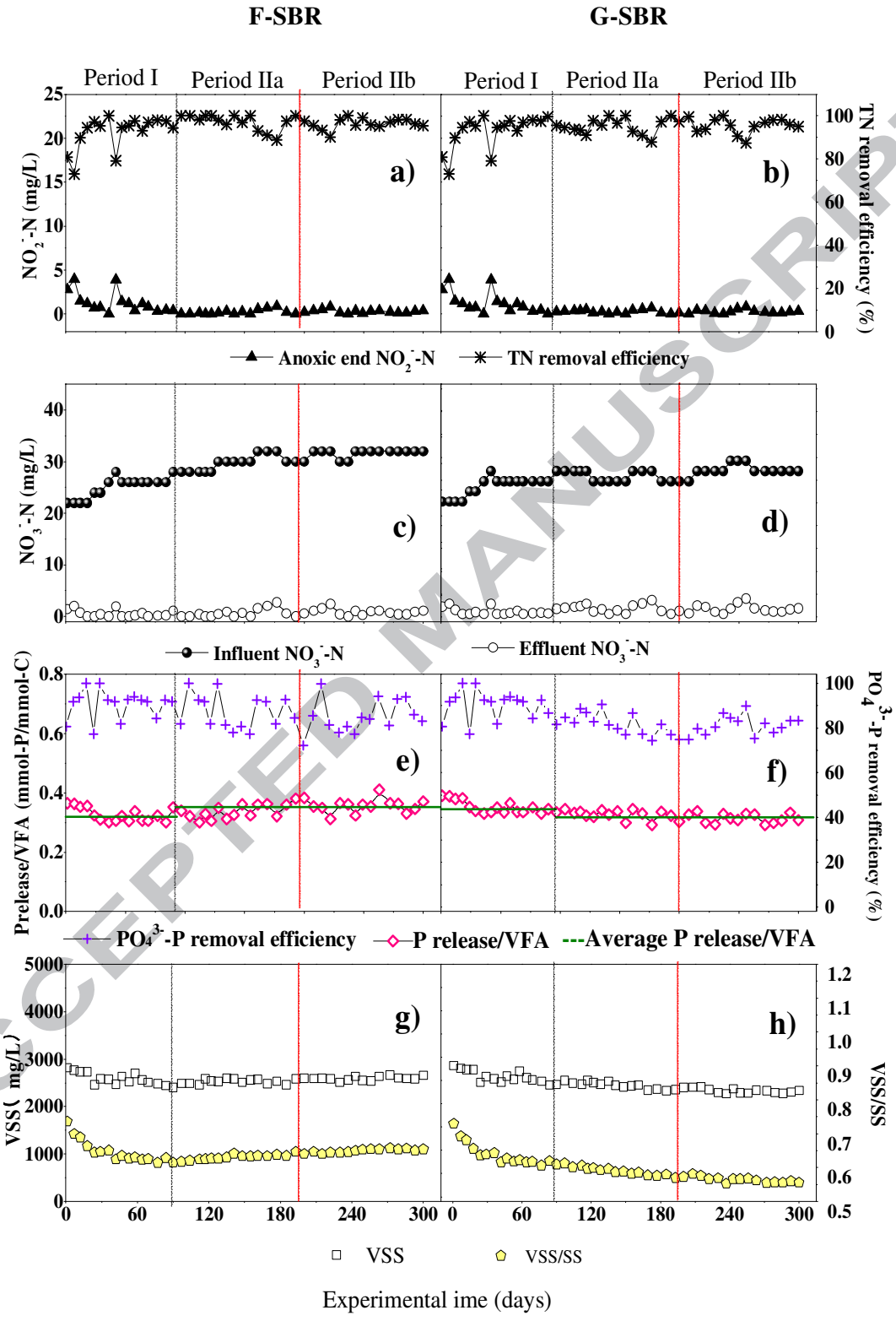

Fig. S2

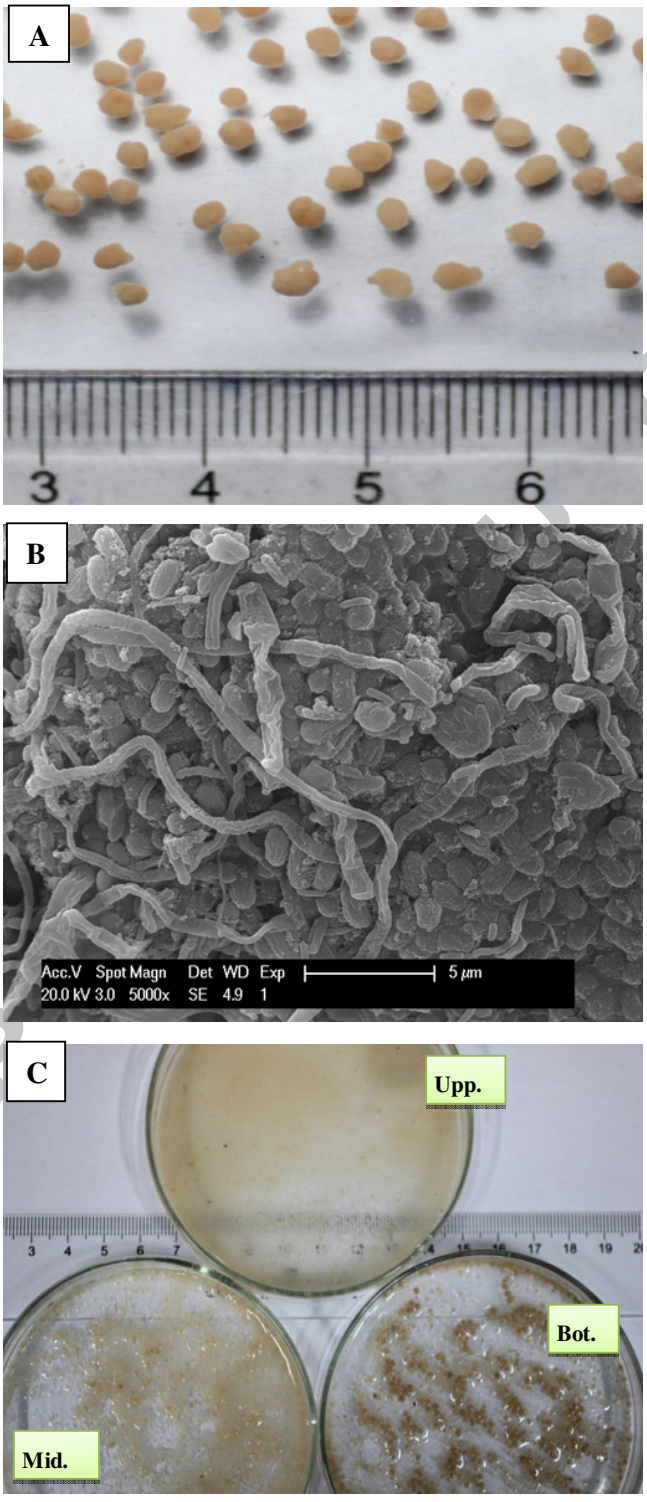

Fig. S3

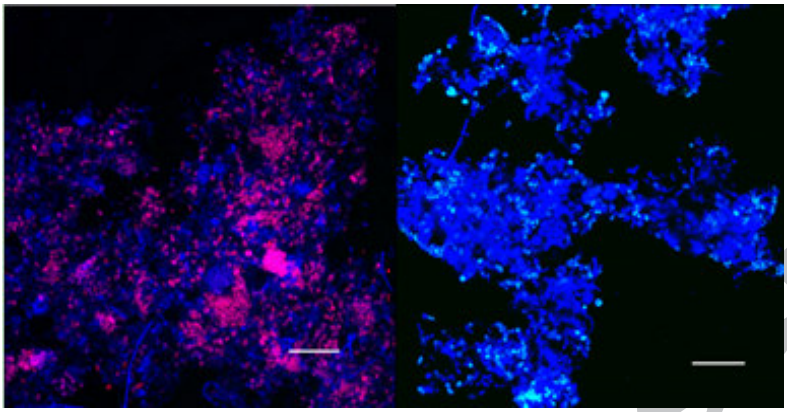

(a) F-SBR

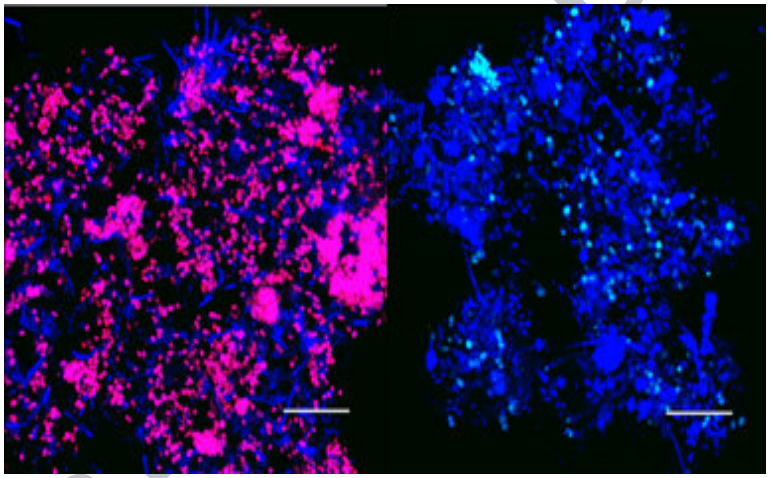

(b) G-SBR

Fig. S4

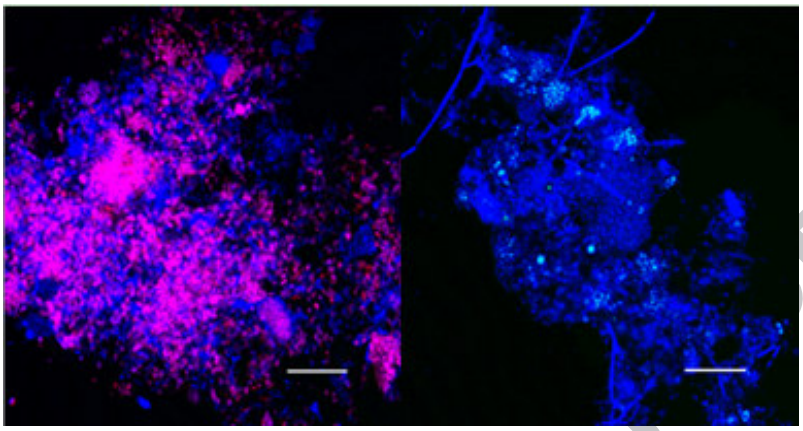

(a) F-SBR

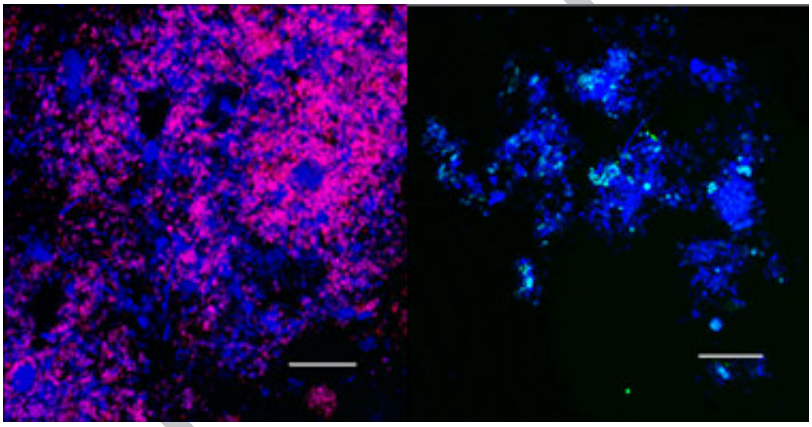

(b) G-SBR

Highlights (maximum 85 characters)

► Denitrifying P removal and nitrite tolerance was compared between flocs and granules

► Granules had higher resistance to nitrite/FNA due to the mass transfer resistance

► Granular sludge had a higher PAOs content than flocs sludge

► PAOII dominated in both systems and performed anoxic P removal cooperated with DGAOs

► PAOs and GAOs existed in different depths in granules

Graphical Abstract